

UniCtrl: Improving the Spatiotemporal Consistency of Text-to-Video Diffusion Models via Training-Free Unified Attention Control

Xuweiyi Chen^{1,2*}, Tian Xia^{2*}, and Sihan Xu^{1,2†}

¹ PixAI.art

² University of Michigan, Ann Arbor
six@mewtant.io

Abstract. Video Diffusion Models have been developed for video generation, usually integrating text and image conditioning to enhance control over the generated content. Despite the progress, ensuring consistency across frames remains a challenge, particularly when using text prompts as control conditions. To address this problem, we introduce **UniCtrl**, a novel, plug-and-play method that is universally applicable to improve the spatiotemporal consistency and motion diversity of videos generated by text-to-video models without additional training. UniCtrl ensures semantic consistency across different frames through cross-frame self-attention control, and meanwhile, enhances the motion quality and spatiotemporal consistency through motion injection and spatiotemporal synchronization. Our experimental results demonstrate UniCtrl’s efficacy in enhancing various text-to-video models, confirming its effectiveness and universality.

Keywords: Video Diffusion · Spatiotemporal Consistency · Attention

1 Introduction

Diffusion Models (DMs) have achieved great success in the field of image generation, demonstrating enhanced stability and superior quality compared to other generative models. Early works on DMs [19, 25, 31, 46–48] have laid the foundation for their success. These models have shown their capacity to efficiently handle and scale to diverse data, outperforming previous generative models like GANs [12, 26, 27] and VAEs [29, 41, 55] in generating images with greater stability and more impressive visual quality.

Furthermore, the evolution of DMs has introduced a significant improvement in terms of controllability and user-interactability in image generation. This progress is highlighted by the recent advancements [34, 36, 40, 42, 43, 65, 67]. These models unleash controllability through various forms of conditions, which

*Authors contributed equally to this work.

†Corresponding author and project lead.



Fig. 1: UniCtrl for Video Generation. we propose **UniCtrl**, a concise yet effective method to significantly improve the temporal consistency of videos generated by diffusion models yet also preserve the motion. UniCtrl requires no additional training and introduces no learnable parameters, and can be treated as a plug-and-play module at inference time.

significantly improves user interactability, allowing for the creation of images that are more aligned with user intentions.

Recently, Video Diffusion Models (VDMs) [20] have been proposed for applying DMs to video generation tasks. With the help of text encoders [39], VDMs are capable of generating videos with a diverse range of motions in text-to-video synthesis tasks [1, 2, 16, 18, 22, 66]. Many open-source text-to-video models have been introduced, including ModelScope [58], AnimateDiff [16], VideoCrafter [6] and so on. These models typically require a pre-trained image generation model, and introduce additional temporal or motion modules. However, unlike images that contain rich semantic information, text conditions are more difficult to ensure consistency between different frames of the generated video. At the same time, some work also uses image conditions to achieve image-to-video generation with improved spatial semantic consistency [1, 15, 23]. Some works have proposed the paradigm of text-to-image-to-video [11], but image conditions alone cannot effectively control the motion of videos. Combining text and image conditions leads to enhanced spatio-temporal consistency in a text-and-image-to-video workflow [6, 7, 14, 62, 68], but these methods require additional training.

To this end, our research goal in this work is to develop an effective plug-and-play method that is training-free, and can be applied to various text-to-video models to improve the performance of generated videos. To solve this problem, we first attempt to ensure that the semantic information between each frame of the video is consistent in principle. This principle draws inspiration from some previous research in attention-based control [4, 17, 54, 64]. These works have

demonstrated in DMs that the queries in attention layers determine the spatial information of the generated image, and correspondingly, values determine the semantic information. We observe that this finding also holds in VDMs and propose the cross-frame self-attention control method. We thus apply the keys and values of the first frame in self-attention layers to each frame and achieve satisfying consistency in the generated video.

Secondly, we observe that as the video’s consistency improves, the motions within videos tend to become less pronounced. To solve this problem, we propose the motion injection mechanism. Based on the assumption that queries control spatial information [4], we divide the sampling process into two branches, namely, an output branch for cross-frame self-attention control, and a motion branch without any attention control. We reserve the queries in the motion branch as motion queries, and use the corresponding motion queries in the output branch. Through the cross-frame self-attention control and motion injection, we ensure that the semantic information between each frame of the video is consistent, while the motion is preserved.

Lastly, we note that motion queries cannot guarantee the spatio-temporal consistency of video. Observing that the output of the output branch has a better spatiotemporal consistency, we further propose the spatiotemporal synchronization, that is, before each sampling step, the latent of the output branch is copied as the initial value of the latent of the motion branch. Our UniCtrl framework combines the above three methods into a plug-in-and-play method that can improve the quality of spatiotemporal consistency and motion quality of the generated videos, while ensuring the consistency of the semantic information of each frame of the video. Through experiments, several text-to-video models have been improved after applying the UniCtrl method, proving the effectiveness and universality of UniCtrl. As illustrated in Fig. 1, UniCtrl plays a significant role in improving spatiotemporal consistency and preserving motion dynamics of generated frames. This method can be readily applied during inference without the need for parameter tuning.

2 Related Work

Video Generation Many previous efforts have explored the task of video generation, e.g., GAN-based models [3, 45, 53] and transformer-based models [21, 57, 59, 60]. Recently, following that Diffusion models (DMs) [19, 25, 31, 46–48] have achieved remarkable results in image generation [35, 36, 40, 42, 43], video diffusion models (VDMs) [20] has also demonstrated their capabilities in video generation [2, 6, 7, 11, 14, 16, 18, 22, 44, 58, 62, 66]. At present, VDMs are mainly implemented by adding additional temporary layers to 2D UNet, which leads to a lack of cross-frame constraints in the training process of the 2D UNet model. Some methods [13, 38, 61] tried to use a training-free method to make the generated videos more smooth. However, how to maintain the cross-frame consistency in videos generated by VDMs remains unresolved.

Attention Control in Diffusion Models Different from models that require training [34, 65, 67], attention control [4, 9, 17, 54, 64] is a training-free method which has been widely applied in the task of image editing. Previous work has found that Attention Control can be used to ensure both semantic [4] and spatial consistency [9, 17, 54] in image editing. InfEdit [64] unified the control of semantic consistency and spatial consistency for the first time, proposing unified attention control (UAC). Some work has introduced attention control to VDMs for video editing [10, 28, 30], but no one has improved the consistency of generated videos by this method. Is that possible to introduce UAC into VDMs to ensure cross-frame semantic consistency and spatial consistency throughout the video is an interesting and worthwhile question to explore.

3 Preliminary

3.1 Diffusion Models (DMs)

Diffusion Models (DMs) [19, 25, 47, 48] are a type of generative model trained via score matching [24, 32, 49, 50]. The forward process gradually adds noise to data to make it follow the Gaussian distribution: $z_t = \mathcal{N}(z_t; \sqrt{\bar{\alpha}_t}z_0, (1 - \sqrt{\bar{\alpha}_t})I)$, where z_0 are samples from the data distribution and $\alpha_1, \dots, \alpha_T$ are from a variance schedule. In [19], this process is re-parameterized into the following form:

$$z_t = \sqrt{\bar{\alpha}_t}z_0 + \sqrt{1 - \bar{\alpha}_t}\varepsilon, \varepsilon \sim \mathcal{N}(0, I) \quad (1)$$

The training objective of DMs is predict the added noise via a neural network ε_θ , to reconstruct the original input from the noisy sample by minimizing the distance $d(\cdot, \cdot)$:

$$\min_{\theta} \mathbb{E}_{z_0, \varepsilon, t} [d(\varepsilon - \varepsilon_\theta(z_t, t))] \quad (2)$$

The sampling process of DMs [19, 47] is iterative and can be represented in the form with different noise schedule σ_t :

$$\begin{aligned} z_{t-1} = & \sqrt{\bar{\alpha}_{t-1}} \left(\frac{z_t - \sqrt{1 - \bar{\alpha}_t} \varepsilon_\theta(z_t, t)}{\sqrt{\bar{\alpha}_t}} \right) & (\text{predicted } z_0) \\ & + \sqrt{1 - \bar{\alpha}_{t-1} - \sigma_t^2} \cdot \varepsilon_\theta(z_t, t) & (\text{direction to } z_t) \\ & + \sigma_t \varepsilon & (\text{random noise}) \end{aligned} \quad (3)$$

Latent Diffusion Models (LDMs) [42] encodes samples into latents using an encoder \mathcal{E} , such that $z_0 = \mathcal{E}(x_0)$. Also, the output is reconstructed via a decoder \mathcal{D} , represented by $\mathcal{D}(z)$. This approach has led to improvements in stability and efficiency in the training and generation process.

Video Diffusion Models (VDMs) [20] extended the application of DMs to the domain of video generation, adapting the framework to handle 4D video tensors in the form of $\text{frames} \times \text{height} \times \text{width} \times \text{channels}$, which we can use z_t^f to describe the frame $f + 1$ at the timestep t .

3.2 Attention Control

We follow the notation from [17, 64]. In the fundamental unit of the diffusion UNet model, there are two main components: cross-attention and self-attention blocks. The process begins with the linear projection of spatial features to generate queries (Q). In the self-attention block, both keys (K) and values (V) are derived from the spatial features through linear projection. Conversely, for the cross-attention part, text features undergo a linear transformation to form keys (K) and values (V). The attention mechanism [56] can be described as:

$$\text{ATTENTION}(Q, K, V) = \text{MV} = \text{softmax}\left(\frac{QK^T}{\sqrt{d}}\right)V \quad (4)$$

Mutual Self-Attention Control (MasaCtrl) is proposed by [4], and find that replacing the Q s in attention layers while keeping the K s and V s same, can change the spatial information of generated images but keeping the semantic information preserved. This technique can help diffusion in spatial-level editing, e.g. a sitting dog to a running dog. Here we use $(\cdot)^{\text{src}}$ to represent the tensor obtained from the source image and $(\cdot)^{\text{tgt}}$ for the target output we want, we can use the following formula to define the MasaCtrl algorithm.

$$\text{out} = \text{ATTENTION}(Q^{\text{tgt}}, K^{\text{src}}, V^{\text{src}})$$

Cross-Attention Control (P2P) is a method mentioned in [17], which is for semantic-level image editing (e.g. dog to cat). This work observed that different V s from different text prompts decide the semantic information of generated images. If attention maps (M) in cross-attention layers have been reserved, but use different V s for the attention calculation, most of the spatial information will be preserved. We here use $(\cdot)^{\text{src}}$ to represent the tensor obtained from the source image and prompt and $(\cdot)^{\text{tgt}}$ for the target output with target prompt, this algorithm can be described as following as same $Q^{\text{src}}, K^{\text{src}}$ lead to same M^{src} :

$$\text{out} = \text{CROSSATTENTION}(Q^{\text{src}}, K^{\text{src}}, V^{\text{tgt}})$$

4 UniCtrl: Cross-Frame Unified Attention Control

In the text-to-video task, it is difficult to ensure the consistency between different frames of the generated video due to the lack of semantic level conditions and the constraint of different frames in the 2D UNet layers. Based on the previous work of DMs [4, 17, 54, 64], it is found that the queries in the attention layers determine the spatial information of the generated images, and correspondingly, the values determine the semantic information. We assume these properties still exist in VDMs.

We first analyzed the role of keys and values in the self-attention layers of VDMs, and then analyzed the role of queries in all the attention layers. Inspired by InfEdit [64], we then propose the cross-frame unified attention control to achieve both semantic level consistency and better spatiotemporal consistency.



Fig. 2: Each row contains 6 frames of videos generated with the same prompt: An Aston Martin is moving. The first row demonstrates the original frames generated with baseline model, which the vehicle and the road are clearly inconsistent across the frames. The second row shows frames generated with baseline model augmented with Cross-Frame Self-Attention Control (SAC). While it maintains semantic consistency, it exhibits little motion. The third row explains frames generated with baseline model augmented with SAC and Motion Injection (MI). Although SAC and MI ensure motion diversity and semantic consistency for each frame, they fall short on spatiotemporal consistency. The fourth row contains frames generated with baseline model and also augmented with Spatiotemporal Synchronization (SS), which improves spatiotemporal consistency over prior pipeline and achieved balance between motion and semantic, both in-frame and cross-frame.

Lastly, we apply spatiotemporal synchronization by replacing the latent of the motion branch with the latent from the output branch at each sampling step. We have demonstrated the effectiveness of each module of UniCtrl in Fig. 2.

4.1 Cross-Frame Self-Attention Control

Previous work [4, 17, 54, 64] has observed that queries in the attention mechanism form the layout and semantic information of generated images [4, 54, 64], while values contribute to the semantic information [17, 64]. Therefore, we hypothesize that using the same values in the attention of different frames can ensure cross-frame consistency. Additionally, we observed that the mismatch between keys

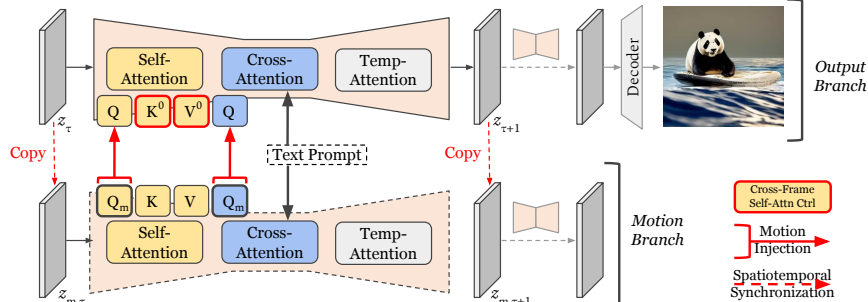


Fig. 3: In our framework, we use key and value from the first frame as represented by K^0 and V^0 in the self-attention block. We also use another branch to keep the motion query Q_m for motion control. At the beginning of every sampling step, we let the motion latent equal to the sampling latent, to avoid spatial-temporal inconsistency.

and values will degrade the quality of generated videos through our experiment and we provide one qualitative example in Section 5.4. Consequently, in our cross-frame **Self-Attention Control** (SAC), we inject both keys and values, as detailed in Algorithm 1. We also show one example of the effectiveness of SAC in Fig. 2.

Algorithm 1 Cross-Frame Self-Attention Control

```

1: Input: Hidden State  $z$ 
2:  $bs, c, f, h, w = z.shape()$ 
3:  $z^0 = z[:, :, 0, :, :].unsqueeze(2)$  # Extract the first frame.
4:  $z^0 = z^0.repeat(1, 1, f, 1, 1)$ 
5:  $Q = \text{to\_q}(z)$ 
6:  $K^0 = \text{to\_k}(z^0)$  # Obtain the Key of the first frame.
7:  $V^0 = \text{to\_v}(z^0)$  # Obtain the Value of the first frame,
8:  $out = \text{SELFATTENTION}(Q, K^0, V^0)$ 
9: Output:  $out$ 

```

4.2 Motion Injection

Through our experiments in section 5, we find one key limitation of cross-frame self-attention control that may lead to overly similar frames, resulting in minimal motion in the video. Again, as described in [4, 64], the queries in self-attention and cross-attention determine the video’s spatial information, which corresponds to motion. Therefore, by preserving the original queries, we can maintain the motion effect. As Fig. 3, we have divided the inference process into two branches: the output branch, which undergoes cross-frame self-attention control, and the motion branch, which does not involve attention control. We retain the queries in the motion branch as motion queries and use the corresponding motion queries in the output branch. Here, we denote motion queries

as Q_m . The method for motion injection can be expressed by the following formula: $out = \text{ATTENTION}(Q_m, \cdot, \cdot)$, where ATTENTION refers to both of self- and cross-attention layers. We implement two methods for motion control: 1) fully preserve the motion of the original video and 2) only preserve the motion during each step of the sampling process. To make motion more controllable, we also introduce a method to control motion through a given motion injection degree c where $0 \leq c \leq 1$, as following:

$$out = \begin{cases} \text{ATTENTION}(Q_m, \cdot, \cdot) & t \geq (1 - c) \times T \\ \text{ATTENTION}(Q, \cdot, \cdot) & t < (1 - c) \times T \end{cases}$$

4.3 Spatiotemporal Synchronization

In our experiments 5, we find that the spatial information of the original video cannot ensure spatiotemporal consistency. Considering that the output of the output branch has better spatiotemporal consistency, we further propose **Spatiotemporal Synchronization (SS)**: the latent of the output branch is copied as the initial value of the latent for the motion branch before each sampling step. By doing so, our method can simultaneously ensure the semantic consistency of the generated video and improve the quality of spatiotemporal consistency and motion.

Algorithm 2 Cross-Frame Unified Attention Control

```

1: Input:
    Video Diffusion Model VDM
    Sequence of timesteps  $\tau_0 > \tau_1 > \dots > \tau_N$ 
    Text Condition  $c$ 
    Controlled Self Attention Algorithm SELFATTNCTRL
    Timestep condition for Motion Control  $t$ 
2:  $z_{m, \tau_0} = z_{\tau_0} \sim \mathcal{N}(\mathbf{0}, \mathbf{I})$ 
3: VDM.SELFATTN = SELFATTNCTRL
4: for  $n = 0$  to  $N - 1$  do
5:    $z_{m, \tau_n} = z_{\tau_n}$ 
6:    $Q_m \leftarrow \mathbf{VDM}(z_{m, \tau_n}, c, \tau_n)$ 
7:   if  $t \geq \tau_n$  then
8:      $z_{\tau_{n+1}} = \mathbf{VDM}(z_{\tau_n}, c, \tau_n) \{Q \leftarrow Q_m\}$ 
9:   else
10:     $z_{\tau_{n+1}} = \mathbf{VDM}(z_{\tau_n}, c, \tau_n)$ 
11:   end if
12: end for
13: Output:  $z_{\tau_N}$ 

```

4.4 Cross-Frame Unified Attention Control

As shown in Fig. 3, we combine the cross-frame unified attention control with motion injection and spatiotemporal synchronization together like Unified At-

tention Control (UAC) in InfEdit [64]. In the output branch, we use the key K^0 and value V^0 from the first frame to ensure cross-frame semantic consistency. We use another branch to keep the reserved query for motion control, and use the query Q_m from this branch to replace the query in the output branch. Before every step of sampling, we let the latent of motion branch equal to the previous output latent, to avoid spatiotemporal inconsistency. Our method can also be represented as formulated algorithm outlined in Algorithm 2.

5 Experiments

In this section, we evaluate the effectiveness of UniCtrl. The assessment includes both qualitative comparisons in Section 5.2 and quantitative comparisons in Section 5.3. Additionally, we explore the contribution of each component within UniCtrl, the motion injection degree, and the specific design choice of swapping Key and Value in the SAC procedure, as detailed in Section 5.4.

5.1 Experimental Setup

To evaluate the effectiveness of our model, we collect prompts from two datasets UCF-101 [51] and MSR-VTT [63] for generating videos. Following Ge et al [8], we use the same UCF-101 prompts for our experiments. We also randomly select 100 unique prompts from the MSR-VTT dataset for our evaluation. Those two parts of data consist of our dataset for evaluations.

Metric To quantitatively evaluate our results, we consider standard metrics following [44, 61]. Note that we will provide details for evaluation metrics in the supplementary material section.

- *DINO*: To evaluate the spatiotemporal consistency in the generated video, we employ DINO [37] to compare the cosine similarity between initial frame and subsequent frames. In our experiments, we utilize the DINO-vits16 [5] model to compute the DINO cosine similarity.
- *RAFT*: To compare the magnitude of actions in the videos, we utilize RAFT [52] to estimate the optical flow, thereby inferring the degree of motion. To quantify the motion intensity between every two consecutive frames, we employ the RAFT model to estimate optical flow for each pixel. We calculate the magnitude of all pixel optical flow using the l^2 norm, and finally, we obtain the average of all magnitude as the score for every consecutive frames in the video. In this process, we utilize the RAFT model from torchvision [33].

Backbones Since our method is plug-and-play, we decide to evaluate our methods on a few popular baselines:

- *AnimateDiff* [16] introduces a practical framework for adding motion dynamics to personalized text-to-image models, such as those created by Stable Diffusion, without the need for model-specific adjustments. Central to AnimateDiff is a motion module, trainable once and universally applicable across personalized

text-to-image models derived from the same base model, leveraging transferable motion priors from real-world videos for animation.

- *VideoCrafter* [6] introduces two novel diffusion models for video generation: T2V, which synthesizes high-quality videos from text inputs, achieving cinematic-quality resolutions up to 1024×576 , and I2V, the first open-source model that transforms images into videos while preserving content, structure, and style. Both models represent significant advancements in open-source video generation technology, offering new tools for researchers and engineers. We use T2V version in our experiments.

Baseline We select FreeInit [61] as our baseline since FreeInit is a training free method that attempts to improve subject appearance and temporal consistency of generated videos through iteratively refining the spatial-temporal low-frequency components of the initial latent during inference. However, given that our method UniCtrl operates on the attention mechanism and FreeInit adjusts the frequency domain of the latent space, UniCtrl and FreeInit are orthogonal approaches. Both are training-free methods capable of enhancing the spatiotemporal consistency of generated videos via diffusion models. We demonstrates the integration of UniCtrl and FreeInit both in 5.2 and 5.3.

5.2 Quatitative Comparisons

Qualitative comparisons, depicted in Figure 4, reveal that our UniCtrl method markedly improves spatiotemporal consistency and maintains motion diversity. For example, with the text prompt "walking with a dog", FreeInit produces inconsistent appearances for both the lady and the dog, whereas UniCtrl ensures consistent representations of both entities. Furthermore, when processing the prompt "A young woman walks through flashing lights", UniCtrl maintains the detailed features of the young woman's dress while ensuring her walking motion remains natural, in contrast to the vanilla AnimateDiff model. Additionally, we demonstrate UniCtrl's flawless integration with FreeInit, enhancing motion in the background while consistently preserving the young woman's appearance. Additional qualitative findings can be found in the supplementary material.

5.3 Quanlitative Comparisons

For quantitative comparisons, the quantitative results on UCF-101 and MSR-VTT are reported in Table 1. We compare the backbones and backbones augmented by UniCtrl and FreeInit respectively. According to the metrics, UniCtrl significantly improves the spatiotemporal consistency in the generated videos across all backbones on both prompt sets from 0.74 to 2.35. While FreeInit achieves remarkable improvements over spatiotemporal consistency, we found that UniCtrl outperforms FreeInit on the diversity of motion for both AnimateDiff and VideoCrafter by a large margin from 10.91 to 21.88. Note that we purposely choose the motion injection degree $c = 1$ to demonstrate how UniCtrl can preserve the motion compare with FreeInit. However, there still exists



Fig. 4: Qualitative Comparisons. We showcase UniCtrl’s adaptability to varied text prompts, leveraging UniCtrl to significantly improve temporal consistency and preserve motion diversity. Comparative inference results with FreeInit are presented for context. Additionally, we demonstrate UniCtrl’s seamless integration with FreeInit.

Table 1: Quantitative Comparisons on UCF-101 and MSR-VTT. UniCtrl significantly improves the temporal consistency while keeps the motion in the generated videos. c indicates the motion injection degree. I indicates number of iteration being used for FreeInit.

| Method | DINO (\uparrow) | RAFT (\uparrow) |
|---|---------------------------|---------------------------|
| AnimateDiff [16] | 93.99 | 31.38 |
| FreeInit + AnimateDiff ($I = 3$) | 96.15 | 14.79 |
| UniCtrl + AnimateDiff ($c = 1$) | 96.34 _(+00.19) | 25.70 _(+10.91) |
| VideoCrafter [6] | 93.39 | 28.25 |
| FreeInit + VideoCrafter ($I = 3$) | 96.61 | 6.90 |
| UniCtrl + VideoCrafter ($c = 1$) | 94.13 _(-02.48) | 28.78 _(+21.88) |
| UniCtrl + FreeInit + AnimateDiff ($I = 3, c = 1$) | 96.48 | 17.91 |

a trade off between spatiotemporal consistency and motion diversity. In section 5.4, we show spatiotemporal consistency can be further improved with a smaller motion injection degree. Thus, we recommend motion injection degree $c = 0.4$ in real-world applications. Lastly, we showcase how UniCtrl and FreeInit can improve AnimateDiff together and we found this integration can improve both spatiotemporal consistency and motion diversity. For the details of our experiments, especially how we integrate UniCtrl and FreeInit, we will introduce the details in the supplementary material. Note that we obtained different score for FreeInit because we randomly sampled a different set of prompts from MSR-VTT. Moreover, we used our own implementations for FreeInit while conducting experiments on VideoCrafter since we cannot find official implementation.

5.4 Ablation Study

We assess the impact of each UniCtrl module, the efficacy of motion injection degree, and corroborate our design choice of swapping Key and Value during SAC through the subsequent ablation studies.

Evaluating the Impact of SAC, MI, and SS To assess the contribution of the Spatial Attention Component (SAC), we conducted experiments on both datasets using AnimateDiff as the baseline, incorporating our pipeline but disabling SAC. For motion injection, we set motion injection degree to be 1. The findings reveal our method without SAC works exactly the same the backbone because the motion branch is the exactly the same as the output branch. This observation underscores the critical role of SAC in enhancing spatiotemporal consistency, as evidenced by the comparisons with the scores obtained through the vanilla AnimateDiff.

In exploring the significance of Motion Injection (MI), additional tests were performed on both datasets with AnimateDiff serving as the baseline, this time with MI deactivated. The results indicated a notable consistency with the baseline, yet with a substantial reduction in motion diversity. This was quantitatively

Table 2: Ablation on UCF-101 and MSR-VTT. We ablate each module of UniCtrl and show the effectiveness of them each. c indicates the motion injection degree.

| Method | DINO (\uparrow) | RAFT |
|-------------------------------------|---------------------|-------|
| AnimateDiff [16] | 93.99 | 31.81 |
| UniCtrl w/o SAC + AnimateDiff | 93.99 | 31.81 |
| UniCtrl w/o MI + AnimateDiff | 97.98 | 4.19 |
| UniCtrl w/o SS + AnimateDiff | 93.98 | 31.78 |
| UniCtrl ($c = 0$) + AnimateDiff | 97.98 | 4.19 |
| UniCtrl ($c = 0.2$) + AnimateDiff | 97.36 | 9.73 |
| UniCtrl ($c = 0.4$) + AnimateDiff | 96.62 | 16.15 |
| UniCtrl ($c = 0.6$) + AnimateDiff | 96.41 | 22.14 |
| UniCtrl ($c = 0.8$) + AnimateDiff | 96.34 | 24.60 |
| UniCtrl ($c = 1.0$) + AnimateDiff | 96.34 | 25.70 |

supported by a decrease in the RAFT score from 31.81 to 4.19. Such a marked disparity highlights MI’s vital contribution to maintaining motion diversity.

Finally, the necessity of the Stabilization Strategy (SS) was examined by excluding SS from our pipeline and conducting experiments across both datasets, again using AnimateDiff as the reference point and setting motion injection degree to be 1. The outcomes showed diminished spatiotemporal consistency in comparison to the baseline, while motion diversity was not significantly impacted. These results emphasize the importance of integrating SS into our pipeline, as corroborated by the UniCtrl’s findings presented in Table 1, illustrating the essential role of SS in achieving the desired balance of spatiotemporal consistency and motion diversity.

Influence of Motion Injection Degree To assess the impact of varying degrees of motion injection, we conducted experiments across both datasets using UniCtrl with motion injection degree set at $c = 0$, $c = 0.2$, $c = 0.4$, $c = 0.6$, $c = 0.8$, and $c = 1$. The effects of different motion injection levels are depicted quantitatively in Table 2. As the degree of motion injection escalates, we observed that the DINO score consistently outperforms baseline metrics, and the RAFT score progressively increases. This trend indicates an amplification in motion diversity. We showcase qualitative examples of the influence of motion injection degree in the supplementary material.

Influence of Swapping Key and Value We aim to provide a qualitative example to underscore the importance of simultaneously modifying both key and value, as highlighted in our discussion on the impact of key and value mismatches in Section 4.1. Initially, we alter only the value while maintaining the same key within the Spatial Attention Component (SAC) performing the UniCtrl pipeline. As depicted in the first row of Fig. 5, the panda begins to fade in the subsequent frames, indicating a substantial decrease in the quality of the generated videos with respect to spatiotemporal consistency. This decline is particularly evident when compared to the approach of modifying both the key and value concurrently using the same UniCtrl pipeline.

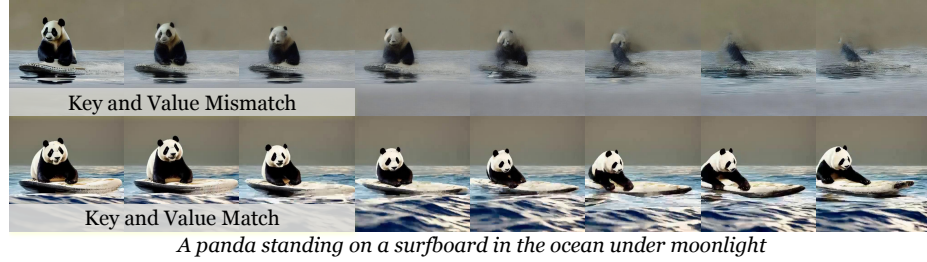


Fig. 5: Each row displays a sequence of video frames generated from the identical prompt: A panda standing on a surfboard in the ocean under moonlight. The section labeled **K and V mismatch** illustrates the frames produced when there is a discrepancy between key and value pairs. Conversely, the section titled **K and V match** showcases frames generated when key and value pairs are in alignment.

6 Conclusion

We introduce Cross-Frame Unified Attention Control (UniCtrl), to address the challenges of cross-frame consistency shift in Video Diffusion Models. By implementing UniCtrl, we've notably improved the alignment of semantic and spatial temporal consistency across frames of generated videos. Our approach stands out as it requires no additional training, making it adaptable to various underlying models. The efficacy of UniCtrl has been rigorously tested, demonstrating its potential to be widely applied to text-to-video generative models. We introduce some key limitations of UniCtrl in section 6.1 and our ethics statement in section 6.2.

6.1 Limitations

Our method needs to operate on the attention mechanism, which limits the application of our method on non-attention-based models. Also, since we ensure the same value for each frame, changing colors within the video is not possible, which limits the model's ability to generate videos. Additionally, we have not yet guaranteed that spatial information is completely consistent across frames; this might be addressed in future work by controlling the temporal attention block. Furthermore, during the inference process, we need additional computation to preserve the motion query, which affects the inference speed. Our method can still be improved by addressing the above issues.

6.2 Ethics Statement

While UniCtrl offers significant advancements in video generation, it is imperative to consider its broader ethical, legal, and societal implications.

Copyright Infringement. As an advanced video generation tool, UniCtrl could be utilized to modify and repurpose original video works, raising concerns over copyright infringement. It is crucial for users to respect the rights of

content creators and uphold the integrity of the creative industry by adhering to copyright and licensing laws.

Deceptive Misuse. Given its ability to generate high-quality, consistent video content, there is a risk that UniCtrl could be exploited for deceptive purposes, such as creating misleading or fraudulent content. This underscores the need for responsible usage guidelines and robust security measures to prevent such malicious applications and protect against security threats.

Bias and Fairness. UniCtrl relies on underlying diffusion models that may harbor inherent biases, potentially leading to fairness issues in the generated content. Although our method is algorithmic and not directly trained on large-scale datasets, it is essential to acknowledge and address any biases present in these foundational models to ensure equitable and ethical utilization.

By proactively addressing these ethical considerations, we can responsibly leverage the capabilities of UniCtrl, ensuring its application aligns with legal standards and societal welfare. Emphasizing ethical practices, legal compliance, and the well-being of society is paramount in advancing video generation technology while maintaining public trust and upholding community values.

7 Acknowledgment

We thank Raven, Tom, Martin, Yichi Zhang, Shengyi Qian for their helpful feedback and advice.

References

1. Blattmann, A., Dockhorn, T., Kulal, S., Mendelevitch, D., Kilian, M., Lorenz, D., Levi, Y., English, Z., Voleti, V., Letts, A., et al.: Stable video diffusion: Scaling latent video diffusion models to large datasets. arXiv preprint arXiv:2311.15127 (2023)
2. Blattmann, A., Rombach, R., Ling, H., Dockhorn, T., Kim, S.W., Fidler, S., Kreis, K.: Align your latents: High-resolution video synthesis with latent diffusion models. In: Proceedings of the IEEE/CVF Conference on Computer Vision and Pattern Recognition. pp. 22563–22575 (2023)
3. Brooks, T., Hellsten, J., Aittala, M., Wang, T.C., Aila, T., Lehtinen, J., Liu, M.Y., Efros, A., Karras, T.: Generating long videos of dynamic scenes. Advances in Neural Information Processing Systems **35**, 31769–31781 (2022)
4. Cao, M., Wang, X., Qi, Z., Shan, Y., Qie, X., Zheng, Y.: Masactrl: Tuning-free mutual self-attention control for consistent image synthesis and editing. In: Proceedings of the IEEE/CVF International Conference on Computer Vision (ICCV). pp. 22560–22570 (October 2023)
5. Caron, M., Touvron, H., Misra, I., Jégou, H., Mairal, J., Bojanowski, P., Joulin, A.: Emerging properties in self-supervised vision transformers (2021)
6. Chen, H., Xia, M., He, Y., Zhang, Y., Cun, X., Yang, S., Xing, J., Liu, Y., Chen, Q., Wang, X., Weng, C., Shan, Y.: Videocrafter1: Open diffusion models for high-quality video generation (2023)

7. Chen, H., Zhang, Y., Cun, X., Xia, M., Wang, X., Weng, C., Shan, Y.: Videocrafter2: Overcoming data limitations for high-quality video diffusion models (2024)
8. Ge, S., Nah, S., Liu, G., Poon, T., Tao, A., Catanzaro, B., Jacobs, D., Huang, J.B., Liu, M.Y., Balaji, Y.: Preserve your own correlation: A noise prior for video diffusion models (2023)
9. Ge, S., Park, T., Zhu, J.Y., Huang, J.B.: Expressive text-to-image generation with rich text. In: IEEE International Conference on Computer Vision (ICCV) (2023)
10. Geyer, M., Bar-Tal, O., Bagon, S., Dekel, T.: Tokenflow: Consistent diffusion features for consistent video editing. arXiv preprint arXiv:2307.10373 (2023)
11. Girdhar, R., Singh, M., Brown, A., Duval, Q., Azadi, S., Rambhatla, S.S., Shah, A., Yin, X., Parikh, D., Misra, I.: Emu video: Factorizing text-to-video generation by explicit image conditioning. arXiv preprint arXiv:2311.10709 (2023)
12. Goodfellow, I., Pouget-Abadie, J., Mirza, M., Xu, B., Warde-Farley, D., Ozair, S., Courville, A., Bengio, Y.: Generative adversarial networks. Communications of the ACM **63**(11), 139–144 (2020)
13. Gu, J., Wang, S., Zhao, H., Lu, T., Zhang, X., Wu, Z., Xu, S., Zhang, W., Jiang, Y.G., Xu, H.: Reuse and diffuse: Iterative denoising for text-to-video generation. arXiv preprint arXiv:2309.03549 (2023)
14. Gu, X., Wen, C., Song, J., Gao, Y.: Seer: Language instructed video prediction with latent diffusion models. arXiv preprint arXiv:2303.14897 (2023)
15. Guo, Y., Yang, C., Rao, A., Agrawala, M., Lin, D., Dai, B.: Sparsectrl: Adding sparse controls to text-to-video diffusion models. arXiv preprint arXiv:2311.16933 (2023)
16. Guo, Y., Yang, C., Rao, A., Wang, Y., Qiao, Y., Lin, D., Dai, B.: Animatediff: Animate your personalized text-to-image diffusion models without specific tuning. arXiv preprint arXiv:2307.04725 (2023)
17. Hertz, A., Mokady, R., Tenenbaum, J., Aberman, K., Pritch, Y., Cohen-or, D.: Prompt-to-prompt image editing with cross-attention control. In: The Eleventh International Conference on Learning Representations (2023), https://openreview.net/forum?id=_CDixzkzeyb
18. Ho, J., Chan, W., Saharia, C., Whang, J., Gao, R., Gritsenko, A., Kingma, D.P., Poole, B., Norouzi, M., Fleet, D.J., et al.: Imagen video: High definition video generation with diffusion models. arXiv preprint arXiv:2210.02303 (2022)
19. Ho, J., Jain, A., Abbeel, P.: Denoising diffusion probabilistic models. Advances in neural information processing systems **33**, 6840–6851 (2020)
20. Ho, J., Salimans, T., Gritsenko, A., Chan, W., Norouzi, M., Fleet, D.J.: Video diffusion models. Advances in Neural Information Processing Systems (2022)
21. Hong, W., Ding, M., Zheng, W., Liu, X., Tang, J.: Cogvideo: Large-scale pretraining for text-to-video generation via transformers. arXiv preprint arXiv:2205.15868 (2022)
22. Hu, Y., Luo, C., Chen, Z.: Make it move: controllable image-to-video generation with text descriptions. In: Proceedings of the IEEE/CVF Conference on Computer Vision and Pattern Recognition. pp. 18219–18228 (2022)
23. Hu, Z., Xu, D.: Videocontrolnet: A motion-guided video-to-video translation framework by using diffusion model with controlnet. arXiv preprint arXiv:2307.14073 (2023)
24. Hyvärinen, A., Dayan, P.: Estimation of non-normalized statistical models by score matching. Journal of Machine Learning Research **6**(4) (2005)

25. Karras, T., Aittala, M., Aila, T., Laine, S.: Elucidating the design space of diffusion-based generative models. *Advances in Neural Information Processing Systems* **35**, 26565–26577 (2022)
26. Karras, T., Laine, S., Aila, T.: A style-based generator architecture for generative adversarial networks. In: *Proceedings of the IEEE/CVF conference on computer vision and pattern recognition*. pp. 4401–4410 (2019)
27. Karras, T., Laine, S., Aittala, M., Hellsten, J., Lehtinen, J., Aila, T.: Analyzing and improving the image quality of StyleGAN. In: *Proc. CVPR* (2020)
28. Khandelwal, A.: Infusion: Inject and attention fusion for multi concept zero-shot text-based video editing. In: *Proceedings of the IEEE/CVF International Conference on Computer Vision*. pp. 3017–3026 (2023)
29. Kingma, D.P., Welling, M.: Auto-encoding variational bayes. In: *International Conference on Learning Representations* (2014)
30. Liu, S., Zhang, Y., Li, W., Lin, Z., Jia, J.: Video-p2p: Video editing with cross-attention control. *arXiv preprint arXiv:2303.04761* (2023)
31. Luo, S., Tan, Y., Huang, L., Li, J., Zhao, H.: Latent consistency models: Synthesizing high-resolution images with few-step inference. *arXiv preprint arXiv:2310.04378* (2023)
32. Lyu, S.: Interpretation and generalization of score matching. *arXiv preprint arXiv:1205.2629* (2012)
33. maintainers, T., contributors: Torchvision: Pytorch’s computer vision library. <https://github.com/pytorch/vision> (2016)
34. Mou, C., Wang, X., Xie, L., Zhang, J., Qi, Z., Shan, Y., Qie, X.: T2i-adapter: Learning adapters to dig out more controllable ability for text-to-image diffusion models. *arXiv preprint arXiv:2302.08453* (2023)
35. Nichol, A.Q., Dhariwal, P.: Improved denoising diffusion probabilistic models. In: *International Conference on Machine Learning*. pp. 8162–8171. PMLR (2021)
36. Nichol, A.Q., Dhariwal, P., Ramesh, A., Shyam, P., Mishkin, P., McGrew, B., Sutskever, I., Chen, M.: Glide: Towards photorealistic image generation and editing with text-guided diffusion models. In: *International Conference on Machine Learning*. pp. 16784–16804. PMLR (2022)
37. Oquab, M., Dariseti, T., Moutakanni, T., Vo, H., Szafraniec, M., Khalidov, V., Fernandez, P., Haziza, D., Massa, F., El-Nouby, A., Assran, M., Ballas, N., Galuba, W., Howes, R., Huang, P.Y., Li, S.W., Misra, I., Rabbat, M., Sharma, V., Synnaeve, G., Xu, H., Jegou, H., Mairal, J., Labatut, P., Joulin, A., Bojanowski, P.: Dinov2: Learning robust visual features without supervision (2024)
38. Qiu, H., Xia, M., Zhang, Y., He, Y., Wang, X., Shan, Y., Liu, Z.: Freenoise: Tuning-free longer video diffusion via noise rescheduling. *arXiv preprint arXiv:2310.15169* (2023)
39. Radford, A., Kim, J.W., Hallacy, C., Ramesh, A., Goh, G., Agarwal, S., Sastry, G., Askell, A., Mishkin, P., Clark, J., et al.: Learning transferable visual models from natural language supervision. In: *International conference on machine learning*. pp. 8748–8763. PMLR (2021)
40. Ramesh, A., Dhariwal, P., Nichol, A., Chu, C., Chen, M.: Hierarchical text-conditional image generation with clip latents. *arXiv preprint arXiv:2204.06125* **1**(2), 3 (2022)
41. Ramesh, A., Pavlov, M., Goh, G., Gray, S., Voss, C., Radford, A., Chen, M., Sutskever, I.: Zero-shot text-to-image generation. In: *International Conference on Machine Learning*. pp. 8821–8831. PMLR (2021)

42. Rombach, R., Blattmann, A., Lorenz, D., Esser, P., Ommer, B.: High-resolution image synthesis with latent diffusion models. In: Proceedings of the IEEE/CVF conference on computer vision and pattern recognition. pp. 10684–10695 (2022)
43. Saharia, C., Chan, W., Saxena, S., Li, L., Whang, J., Denton, E.L., Ghasemipour, K., Gontijo Lopes, R., Karagol Ayan, B., Salimans, T., et al.: Photorealistic text-to-image diffusion models with deep language understanding. *Advances in Neural Information Processing Systems* **35**, 36479–36494 (2022)
44. Singer, U., Polyak, A., Hayes, T., Yin, X., An, J., Zhang, S., Hu, Q., Yang, H., Ashual, O., Gafni, O., et al.: Make-a-video: Text-to-video generation without text-video data. *arXiv preprint arXiv:2209.14792* (2022)
45. Skorokhodov, I., Tulyakov, S., Elhoseiny, M.: Stylegan-v: A continuous video generator with the price, image quality and perks of stylegan2. In: Proceedings of the IEEE/CVF Conference on Computer Vision and Pattern Recognition. pp. 3626–3636 (2022)
46. Sohl-Dickstein, J., Weiss, E., Maheswaranathan, N., Ganguli, S.: Deep unsupervised learning using nonequilibrium thermodynamics. In: International conference on machine learning. pp. 2256–2265. PMLR (2015)
47. Song, J., Meng, C., Ermon, S.: Denoising diffusion implicit models. In: International Conference on Learning Representations (2020)
48. Song, Y., Dhariwal, P., Chen, M., Sutskever, I.: Consistency models. *arXiv preprint arXiv:2303.01469* (2023)
49. Song, Y., Ermon, S.: Generative modeling by estimating gradients of the data distribution. *Advances in neural information processing systems* **32** (2019)
50. Song, Y., Sohl-Dickstein, J., Kingma, D.P., Kumar, A., Ermon, S., Poole, B.: Score-based generative modeling through stochastic differential equations. *arXiv preprint arXiv:2011.13456* (2020)
51. Soomro, K., Zamir, A.R., Shah, M.: Ucf101: A dataset of 101 human actions classes from videos in the wild (2012)
52. Teed, Z., Deng, J.: Raft: Recurrent all-pairs field transforms for optical flow (2020)
53. Tian, Y., Ren, J., Chai, M., Olszewski, K., Peng, X., Metaxas, D.N., Tulyakov, S.: A good image generator is what you need for high-resolution video synthesis. *arXiv preprint arXiv:2104.15069* (2021)
54. Tumanyan, N., Geyer, M., Bagon, S., Dekel, T.: Plug-and-play diffusion features for text-driven image-to-image translation. In: Proceedings of the IEEE/CVF Conference on Computer Vision and Pattern Recognition (CVPR). pp. 1921–1930 (June 2023)
55. Van Den Oord, A., Vinyals, O., et al.: Neural discrete representation learning. *Advances in neural information processing systems* **30** (2017)
56. Vaswani, A., Shazeer, N., Parmar, N., Uszkoreit, J., Jones, L., Gomez, A.N., Kaiser, Ł., Polosukhin, I.: Attention is all you need. *Advances in neural information processing systems* **30** (2017)
57. Villegas, R., Babaeizadeh, M., Kindermans, P.J., Moraldo, H., Zhang, H., Saffar, M.T., Castro, S., Kunze, J., Erhan, D.: Phenaki: Variable length video generation from open domain textual description. *arXiv preprint arXiv:2210.02399* (2022)
58. Wang, J., Yuan, H., Chen, D., Zhang, Y., Wang, X., Zhang, S.: Modelscope text-to-video technical report (2023)
59. Wu, C., Huang, L., Zhang, Q., Li, B., Ji, L., Yang, F., Sapiro, G., Duan, N.: Godiva: Generating open-domain videos from natural descriptions. *arXiv preprint arXiv:2104.14806* (2021)

60. Wu, C., Liang, J., Ji, L., Yang, F., Fang, Y., Jiang, D., Duan, N.: Nüwa: Visual synthesis pre-training for neural visual world creation. In: European conference on computer vision. pp. 720–736. Springer (2022)
61. Wu, T., Si, C., Jiang, Y., Huang, Z., Liu, Z.: Freeinit: Bridging initialization gap in video diffusion models. arXiv preprint arXiv:2312.07537 (2023)
62. Xing, J., Xia, M., Zhang, Y., Chen, H., Wang, X., Wong, T.T., Shan, Y.: Dynamicrofaster: Animating open-domain images with video diffusion priors. arXiv preprint arXiv:2310.12190 (2023)
63. Xu, J., Mei, T., Yao, T., Rui, Y.: Msr-vtt: A large video description dataset for bridging video and language (June 2016)
64. Xu, S., Huang, Y., Pan, J., Ma, Z., Chai, J.: Inversion-free image editing with natural language. arXiv preprint arXiv:2312.04965 (2023)
65. Xu, S., Ma, Z., Huang, Y., Lee, H., Chai, J.: Cyclenet: Rethinking cycle consistent in text-guided diffusion for image manipulation. In: Advances in Neural Information Processing Systems (2023)
66. Zhang, D.J., Wu, J.Z., Liu, J.W., Zhao, R., Ran, L., Gu, Y., Gao, D., Shou, M.Z.: Show-1: Marrying pixel and latent diffusion models for text-to-video generation. arXiv preprint arXiv:2309.15818 (2023)
67. Zhang, L., Rao, A., Agrawala, M.: Adding conditional control to text-to-image diffusion models. In: Proceedings of the IEEE/CVF International Conference on Computer Vision. pp. 3836–3847 (2023)
68. Zhang, Y., Xing, Z., Zeng, Y., Fang, Y., Chen, K.: Pia: Your personalized image animator via plug-and-play modules in text-to-image models. arXiv preprint arXiv:2312.13964 (2023)